Quantitative Study of Metachromasy. The Analysis of the Dye–Polyphosphate Multiequilibrium System by the Principal Component Analysis Method

Mineo TAKATSUKI

Faculty of Science, Hiroshima University, Higashisenda-machi, Hiroshima 730

(Received December 26, 1979)

The absorption spectra of three dyes, 9-aminoacridine (AA), Crystal Violet (CV), and Trypaflavine (TF), were measured in the presence of sodium polyphosphate (NaPP). The optical titrations were performed at phosphate residue-to-dye ratios between 26.6 and 2130 for AA, between 42.6 and 788 for CV, and between 53.9 and 1120 for TF. Using a model in which the condensation of dyes to a polyelectrolyte and the bound monomer⇌bound aggregate equilibrium in the vicinity of the polymer are assumed, the extended principal component analysis was applied to the observed spectra of each dye–NaPP system. The equilibrium constants and the pure spectra of bound dye species were determined. Both the bound monomer and the bound dimer were present in the AA–NaPP system, while the bound monomer, bound dimer, and bound tetramer were present in both CV– and TF–NaPP systems. In all the cases, the absorption spectrum of the bound monomer showed a slight bathochromic shift. The absorption spectrum of the bound dimer of AA showed a considerable bathochromic shift without any new band, while the spectrum of the bound dimer and bound tetramer of CV and TF showed metachromasy bands in wavelength ranges both shorter and longer than the peak wavelength of free CV and TF.

An aqueous solution of several dyes in the presence of a polyelectrolyte shows a color change, namely metachromasy, which is affected in various ways by the combination of dyes and polymers.[1–22] Many papers have been published on the interaction between metachromatic dyes and biological polymers including DNA,[4,6,14–22] because most metachromatic dyes show mutagenic effects. In order to investigate the interactions between the dyes and polymers, the measurement of the absorption spectra is a useful method. However, the absorption spectra of a dye-polyelectrolyte solution are generally composed of some absorbing species, whose fractions vary with the change in the molar ratio of the polymer residue to the dye (P/D). Therefore, in order to study the nature of metachromasy quantitatively, the number of absorbing species and the 'pure' spectrum of the species in an equilibrium system of dye and polymer have to be determined.

The method of principal component analysis (the PCA method) was extended to determine not only the number of absorbing species in an equilibrium system, but also the equilibrium scheme among the species and their pure absorption spectra.[23] The PCA method was successfully applied to the equilibrium systems of cationic dyes and various polyanions in the low-P/D region between 0 and 1.[4,5] The presence of two dye species, namely a free and a bound dye, in the low-P/D region was ascertained for those systems. Furthermore, it was predicted that two or more bound dye species are present in the high-P/D region.[5]

The main purpose of this work is to determine the number of bound dye species over a wide P/D region and to determine the equilibrium scheme of the dye–polymer system and the absorption spectrum of the bound-dye species by using the PCA method. It is also interesting to study the effect of the structure of the dye on the metachromasy. Therefore, three different dyes 9-aminoacridine (AA, monoaminoacridine dye), Crystal Violet (CV, triphenylmethane dye), and Trypaflavine (TF, diaminoacridine dye), all of which interact with DNA and show metachromasy,[4,20,21] were chosen as sample dyes. Sodium polyphosphate (NaPP), which can be thought of as a model of the DNA backbone, was chosen as the polymer, because the pure spectrum of the dye species bound to NaPP will give information about distinguishing the interaction between the dye and the ionized group of DNA from that between the dye and the base pair of DNA.

The application of the PCA method to the spectra observed over a wide P/D region revealed that only two bound-dye species are present in the AA–NaPP system and that only three are present in the CV– and TF–NaPP systems. Such results do not agree with the cooperative binding model, which has been used for metachromasy, because that model implies that a large number of bound-dye species are present over a wide P/D region.[9,10,24,25] Hence, a new model was proposed for the metachromasy. In the present model, it was assumed that the dyes are condensed near the polyelectrolyte and aggregate in its vicinity. Then, the equilibrium constants among the bound-dye species and their pure spectra were determined by the extended PCA method.

Experimental

Materials. The preparation of AA was reported elsewhere.[26] The dyes of CV and TF are the same samples as were reported previously.[4] The NaPP samples (with number-average degrees of polymerization, $\bar{n}$, of 154 and 158) used in this work are the same refractionated preparations as have been described elsewhere.[2] The difference in the degree of polymerization of the two NaPP's did not affect the metachromasy for CV and TF.[2,3]

Procedure. A series of absorption spectra of a dye solution were measured by titrating it with an NaPP solution delivered through a micrometer buret (Gilmont). The volume change in the titrate was made smaller than 10% so as not to shift the binding equilibrium. The concentration of the dye solution was optically determined immediately before the addition of the NaPP solution from the molar absorption coefficient: 1.03×10^4 at 401 nm for AA, 9.20×10^4 at 592 nm for CV, and 4.67×10^4 at 452 nm for TF. The initial concentrations of AA, CV, and TF were 44.3 μM (1 μM = 1×10^{-6} mol dm^{-3}), 8.37 μM, and 9.58 μM re-

spectively. The residue concentrations of the titrant NaPP were 0.847 M ($\bar{n}=158$) for AA and 0.301 M ($\bar{n}=154$) for CV and TF. The absorbances of NaPP in the UV range were subtracted from the observed absorbance of the AA–NaPP system.

Measurements. A Hitachi EPS-3T recording spectrophotometer was used together with matched pair of 1-, 2-, and 5-cm long quartz cells. The temperature of the solution was kept at 25 °C. Other precautions for measurements were described in Ref. 4.

The Extended Principal Component Analysis Method

The PCA method, which is applicable to the family of spectrophotometric data including absorption, CD, and ORD spectra for the determination of the number of components involved in a chemical equilibrium system, was extended to determine the equilibrium scheme, equilibrium constant, and the pure spectrum of components in an equilibrium system.[23,27] A specific application to the multiequilibrium system will be described here, because the description of the general method has been given previously.[4,23,27]

Assume that m observed absorption spectra are measured at n selected wavelengths, λ_j, $j=1\cdots n$. The observed data can be represented as an $m\times n$ matrix, $\boldsymbol{D}$:

$$\boldsymbol{D}=\begin{pmatrix} D_1(\lambda_1)\cdots D_1(\lambda_n) \\ \cdots\cdots\cdots\cdots \\ D_m(\lambda_1)\cdots D_m(\lambda_n) \end{pmatrix}. \tag{1}$$

The number of absorbing species, which are assumed to vary independently, can be determined by the variation in the eigenvalue of the second-moment matrix, $\boldsymbol{A}$, which is constructed by the product of the data matrix, $\boldsymbol{D}$, and its transposed matrix, ${}^t\boldsymbol{D}$: $\boldsymbol{A}={}^t\boldsymbol{D}\boldsymbol{D}$. The eigenvalues and eigenvectors can be calculated by the diagonalization of the $\boldsymbol{A}$ matrix. The magnitude of the eigenvalue represents the contribution of the corresponding eigenvector to the $\boldsymbol{D}$ matrix. In view of the reading error of the observed spectra, if the ratio of a given eigenvalue to the maximum eigenvalue is greater than 10^{-5}, the corresponding eigenvector is thought to be significant. If p eigenvalues satisfy such a condition, one can conclude that the data matrix is composed of p independent principal components. The data matrix can be reconstructed by a linear combination of the p eigenvectors as follows:

$$\boldsymbol{D}=\boldsymbol{f}\boldsymbol{e}=\begin{pmatrix} f_{11}\cdots f_{1p} \\ \cdots\cdots\cdots \\ f_{m1}\cdots f_{mp} \end{pmatrix}\begin{pmatrix} e_{11}\cdots e_{1n} \\ \cdots\cdots\cdots \\ e_{p1}\cdots e_{pn} \end{pmatrix}, \tag{2}$$

where $\boldsymbol{f}$ is the linear combination coefficient matrix and $\boldsymbol{e}$ is the eigenvector matrix. Furthermore, the molar absorption coefficient matrix, $\boldsymbol{\varepsilon}$, which represents the pure spectrum of the p absorbing species, can also be transformed from the p eigenvectors by means of the transformation matrix, $\boldsymbol{t}$: $\boldsymbol{\varepsilon}=\boldsymbol{t}\,\boldsymbol{e}$.[23] The evaluation of the ε's is reduced to the problem of evaluating the $\boldsymbol{t}$ matrix.

According to Beer's law, a $\boldsymbol{D}$ matrix can also be represented by the product of a concentration matrix, $\boldsymbol{C}$, and an $\boldsymbol{\varepsilon}$ matrix: $\boldsymbol{D}=\boldsymbol{C}\,\boldsymbol{\varepsilon}$. Thus, the $\boldsymbol{C}$ matrix is given by the product of an $\boldsymbol{f}$ matrix and an inverse matrix of $\boldsymbol{t}$: $\boldsymbol{C}=\boldsymbol{f}\,\boldsymbol{t}^{-1}$.[23] The $\boldsymbol{f}$ matrix can be calculated from Eq. 2 by the least-squares method. Thus, the $\boldsymbol{C}$ matrix can also be evaluated if the $\boldsymbol{t}$ matrix is given.

The PCA method was extended to evaluate the most probable $\boldsymbol{t}$ matrix by successive examinations of the probable equilibrium equation for an unknown equilibrium system. A general expression for the equilibrium constant among the p absorbing species is:

$$K=\prod_{i=1}^{p}[X_i]^{\nu_i}, \tag{3}$$

where X_i is the ith absorbing component and ν_i is the stoichiometric coefficient of X_i, whose equilibrium concentration is denoted by the brackets. The substitution of the elements of the $\boldsymbol{C}$ matrix into the right-hand side of Eq. 3 yields m different values for K unless the elements of the $\boldsymbol{t}$ matrix and the assumed equilibrium expression are correct. In order to discriminate the most probable $\boldsymbol{t}$ matrix and the equilibrium expression from the remainder, the coefficient of the variation, S, of K is defined by Eq. 4 and used as a criterion:

$$S=\left(\frac{1}{m}\sum_{j=1}^{m}(K_j-\bar{K})^2\right)^{1/2}\Big/\bar{K}, \tag{4}$$

where $\bar{K}$ denotes the mean value of K_j. The elements of the $\boldsymbol{t}$ matrix and the equilibrium expression which yields the minimum S value can be determined by iterative calculations.

In the multiequilibrium system, the values of S are calculated for individual equilibrium constants, and then the mean value of the S's for the equilibrium constants is used as a criterion. In the iterative calculations, the $\boldsymbol{t}$ matrix sometimes gave as the S values some minima where the calculated concentrations and/or ε of absorbing species were negative. Therefore, the most probable $\boldsymbol{t}$ matrix was selected to yield the positive value for the concentrations and to minimize the value of S. In this work, an acceptable upper limit of 0.10 was preset for the minimized value of S in view of the experimental errors.[23] All the calculations were carried out with a HITAC-8700 computer in FORTRAN language.

Results

Absorption Spectra of AA–, CV–, and TF–NaPP Systems. The absorption spectra of dye–NaPP systems over a wide P/D region were measured in order to obtain significant information on the metachromasy by the use of the extended PCA method. The absorption spectra of AA were measured in both visible and UV wavelength ranges, because the ^1L_a and ^1L_b bands of free AA are located in visible and UV ranges separately.[21,28] As is shown in Fig. 1(a), the ε's of the four bands of AA in the visible range increase and their positions shift toward shorter wavelengths with the increase in P/D. A few UV absorption spectra of AA are shown in Fig. 1(b). The intensities of the two bands in the UV range also increase, and

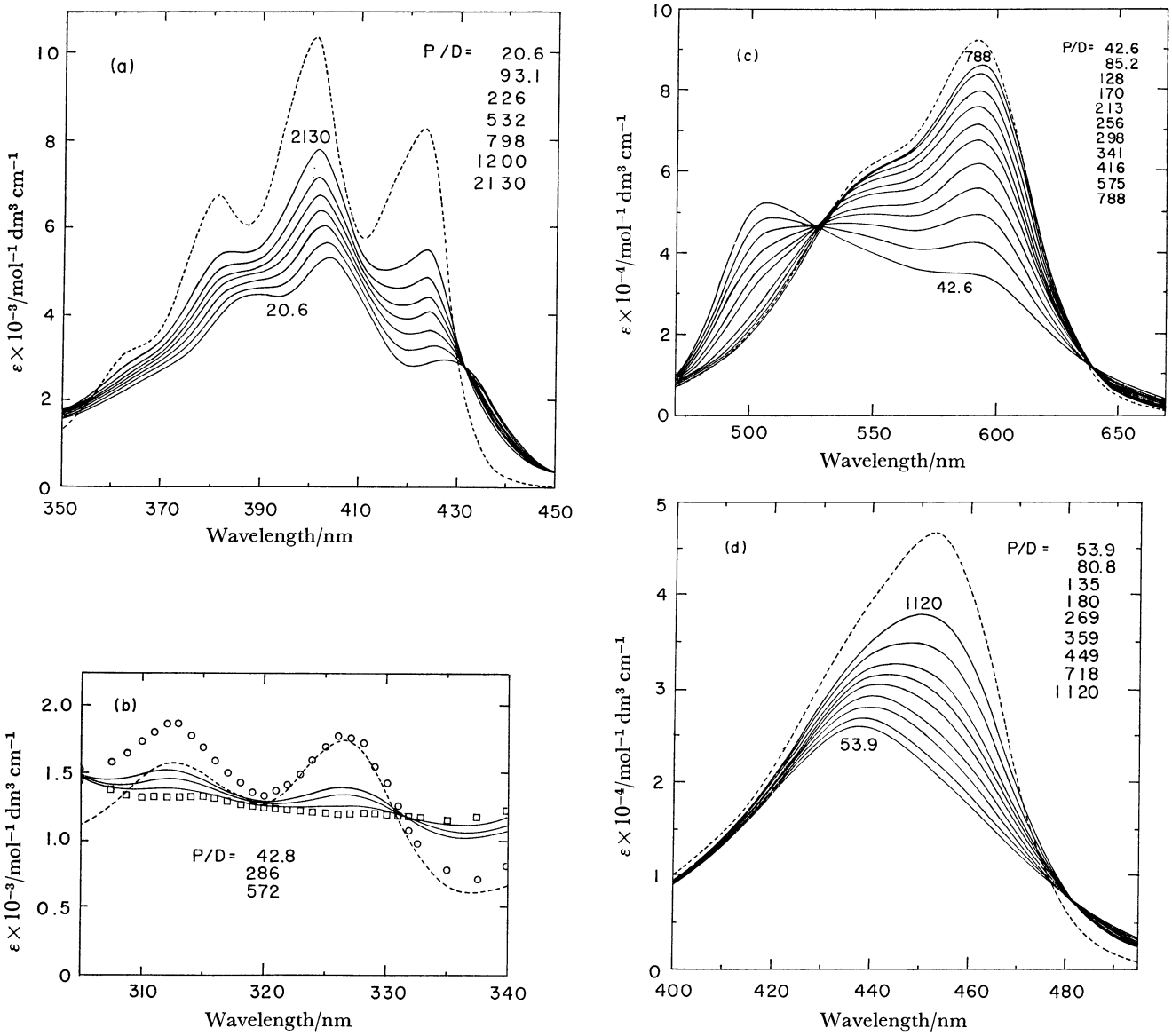

Fig. 1. Visible (a) and UV (b) absorption spectra of AA and visible absorption spectra of CV (c) and TF (d) in the high P/D region.
The concentrations of dyes are: (a) 44.3 μM, (b) 44.3 μM, (c) 8.37 μM, and (d) 9.58 μM. The concentrations of NaPP are listed in each figure in terms of P/D, the order of which corresponds to the order of the increase in the maximum absorbance. Spectrum of free dye is shown by dashed curve in each figure for comparison. Pure spectra of bound monomer (○) and dimer (□) are shown in (b).

TABLE 1. THE POSITIONS OF ISOSBESTIC POINTS

Dye	P/D	Wavelength/nm			
AA	0—1[a)]	306	331	352	428
	26.6—2130	—	—	350	431
CV	0—1[b)]	460	529	639	
	40—150	452	526	636	
TF	0—1[b)]	371	476		
	50—130	374	479		

a) Ref. 29. b) Ref. 4.

their positions shift toward shorter wavelengths with the increase in P/D. Figure 1(c) shows that a remarkable metachromasy band of CV observed at 510 nm gradually disappears and that the ε at the peak position of the free dye spectrum increases with the increase in P/D. In the TF–NaPP system, as is shown in Fig. 1(d), the ε at the absorption peak increases and its position shifts toward longer wavelengths with the increase in P/D.

The positions of the observed isosbestic points and P/D regions, in which the isosbestic points were observed, are listed in Table 1 for each system. In the CV- and TF–NaPP systems, the isosbestic points were observed within a high-P/D region, while those in the AA–NaPP system were observed over a wide P/D region. It is noteworthy that the isosbestic points observed in the high-P/D region differ from those in the low-P/D region in all the cases shown in Table 1. This means that more than two absorbing components are present throughout the P/D region.

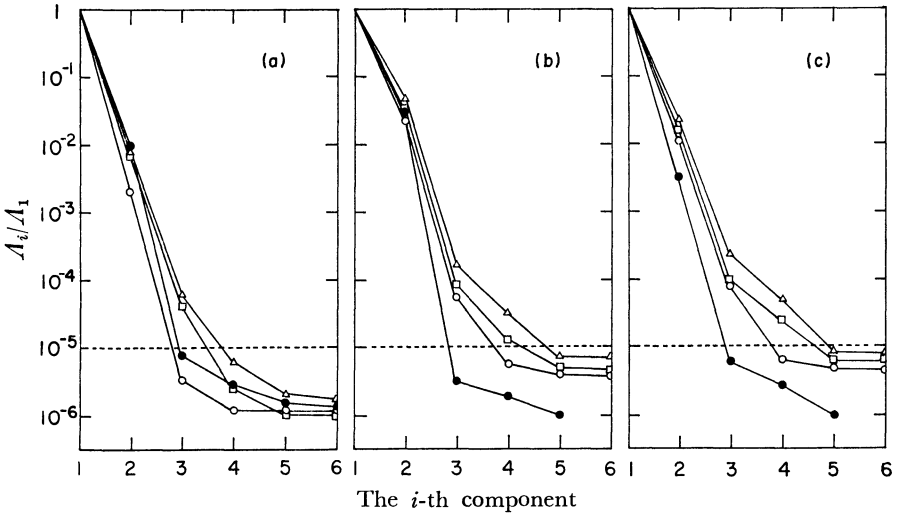

Fig. 2. Variation in eigenvalue Λ_i with the i-th absorbing component for various combinations of observed spectra in the systems of NaPP and AA (a), CV (b), and TF (c). P/D regions of spectra applied the PCA method are; ○: high P/D region ((a) P/D=26.6—2130, (b) 42.6—788, and (c) 53.9—1120), ●: low P/D region ((a) P/D=0—1.02, (b) 0—1.21, and (c) 0—1.25), □: high P/D region and free dye, △: high P/D region and low P/D region. The dashed line indicates the lower limit of the magnitude of eigenvalue for principal component. Selected wavelengths are (a) 48 points from 356 to 450 nm, (b) 50 points from 470 to 666 nm, and (c) 48 points from 400 to 494 nm.

Table 2. The variation in the number of absorbing species with the combination of spectra

Dye	Low P/D	High P/D	Low and high P/D	Free dye and high P/D
AA	2[a)]	2	3	3
CV	2[b)]	3	4	4
TF	2[b)]	3	4	4

a) Ref. 29. b) Ref. 4.

The Number of Absorption Species in AA–, CV–, and TF–NaPP Systems. In order to determine the number of absorbing species in each system, the PCA method was applied to the observed spectra. In each system, four data matrices were analyzed: 1) a set of spectra observed in the high-P/D region, 2) a set of spectra observed in the low-P/D region,[4,29)] 3) a set of spectra observed in both the low- and high-P/D region, and 4) a set of spectra observed in the high-P/D region and the spectrum of a free dye. The variations in the eigenvalues, Λ_i, with the ith component are shown in Figs. 2(a)—(c). The number of absorbing species in each set was determined by the use of the criterion mentioned in the previous section. The results listed in Table 2 show that three absorbing species of AA and four of CV and TF are present in the entire P/D region. In all the systems, the sum of the number of species in the low-P/D region and the number of species in the high-P/D region is greater by one than the number of species in the entire P/D region. That is, there is a common species in the low- and high-P/D regions. Furthermore, the results show that the absorbing species present in the high-P/D region differ from the free dye, because the number of species is increased by the addition of the spectrum of the free dye to the spectra observed in the high-P/D region. Thus, it can be said that two bound-dye species of AA and three of CV and TF are present in the high-P/D region. It can also be said that the amount of free dye in the high-P/D region is negligibly small. Therefore, the presence of the free dye can be neglected in the analysis of the observed data in the high-P/D region.

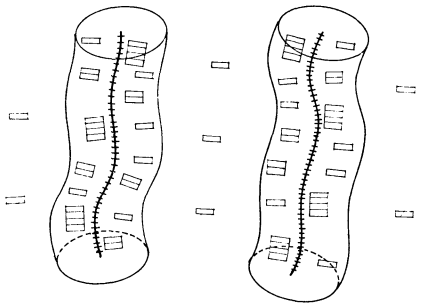

Fig. 3. Schematic model of dye–polyelectrolyte solution.

Equilibrium Scheme among the Bound-dye Species and Their Absorption Spectra. The number of bound-dye species determined in the preceding section is contrary to the number of those expected by the cooperative binding model, which has previously been used for Metachromasy,[9,10,24,25)] as will be discussed later. In this work, a model is used for the distribution of dyes in a polyelectrolyte solution on the basis of the theory for the condensation of the counter ion of a polymer.[30)] As is shown in Fig. 3, dyes in a polyelectrolyte solution are classified into two categories: dyes freely moving outside the region occupied by macroions, and those condensed as bound but mobile ions in the vicinity of the polymer. Assume that the equilibrium of aggregation among the bound

Table 3. Values of S for equilibrium schemes examined

AA		CV				TF		
n	S	Scheme	S	Concn	Spectrum	S	Concn	Spectrum
2	0.075	I	—	posi.	neg.	—	posi.	neg.
3	0.22	II	0.21	posi.	neg.	0.22	posi.	neg.
4	0.52	III	0.09	posi.	posi.	0.09	posi.	posi.
		IV	—	posi.	posi.	—	posi.	neg.

—: $S>1$.

dyes is established inside the region occupied by macroions. Generally, the equilibrium equation for the aggregation can be expressed as follows:

$$n\mathrm{D}_1^b \rightleftharpoons \mathrm{D}_n^b, \tag{5}$$

where D_1^b is the bound monomer dye and D_n^b is the bound n-mer dye. In the vicinity of the polymer, the concentration of the respective bound-dye species may be proportional to the ratio of the amount of dyes to that of the polymer residues. Therefore, the equilibrium constant in the vicinity of the polymer can be represented as:

$$K = \frac{[\mathrm{D}_n^b]/C_p}{([\mathrm{D}_1^b]/C_p)^n} \tag{6}$$

where C_p denotes the total concentration of the polymer residues. In the application of the extended PCA method to the multiequilibrium system, such an expression for the equilibrium constant of the individual equilibrium is convenient for finding the most probable combination of equilibrium equations.

The presence of two bound-dye species in the high-P/D region of the AA–NaPP system was confirmed. Hence, the equations for the aggregation numbers, n, of 2, 3, and 4 were examined on the assumption that a bound-dye species is the bound monomer dye. The values of S, minimized for each n, are listed in Table 3. The minimized value of S for $n=2$ is smaller than the preset upper limit of S and is the smallest in the three cases of $n=2$, 3, and 4. The minimized values of S for $n=3$ and 4 exceed the preset upper limit; therefore, the aggregation number in the AA–NaPP system is two.

In both CV– and TF–NaPP systems, there are three bound-dye species, one of which may be the bound monomer. The following four equilibrium scheme were considered for those systems. As Scheme I, the simplest growth process of aggregation was adopted. The equilibrium equations and equilibrium constants can be expressed as follows:

$$2\mathrm{D}_1^b \rightleftharpoons \mathrm{D}_2^b, \quad K_1 = \frac{[\mathrm{D}_2^b]/C_p}{([\mathrm{D}_1^b]/C_p)^2}, \tag{7}$$

$$\mathrm{D}_1^b + \mathrm{D}_2^b \rightleftharpoons \mathrm{D}_3^b, \quad K_2 = \frac{[\mathrm{D}_3^b]/C_p}{([\mathrm{D}_1^b]/C_p)([\mathrm{D}_2^b]/C_p)}. \tag{8}$$

In Scheme II, the formation of the bound tetramer from two bound dimers was assumed to be as follows:

$$2\mathrm{D}_1^b \rightleftharpoons \mathrm{D}_2^b, \quad K_1 = \frac{[\mathrm{D}_2^b]/C_p}{([\mathrm{D}_1^b]/C_p)^2}, \tag{9}$$

$$2\mathrm{D}_2^b \rightleftharpoons \mathrm{D}_4^b, \quad K_2 = \frac{[\mathrm{D}_4^b]/C_p}{([\mathrm{D}_2^b]/C_p)^2}. \tag{10}$$

Table 4. Equilibrium constants of aggregation among the bond-dye species at 25 °C

Dye	K	K_1	K_2
AA	2.2×10^3		
CV		6.6×10^1	2.8×10^6
TF		2.8×10^2	2.8×10^7

The formation of a bound dimer from two bound monomers and the direct formation of a bound tetramer from four bound monomers were assumed to proceed as in Scheme III:

$$2\mathrm{D}_1^b \rightleftharpoons \mathrm{D}_2^b, \quad K_1 = \frac{[\mathrm{D}_2^b]/C_p}{([\mathrm{D}_1^b]/C_p)^2} \tag{11}$$

$$4\mathrm{D}_1^b \rightleftharpoons \mathrm{D}_4^b, \quad K_2 = \frac{[\mathrm{D}_4^b]/C_p}{([\mathrm{D}_1^b]/C_p)^4} \tag{12}$$

As Scheme IV, the formation of a bound trimer from three bound monomers and the formation of a bound hexamer from two trimers were assumed to proceed as follows:

$$3\mathrm{D}_1^b \rightleftharpoons \mathrm{D}_3^b, \quad K_1 = \frac{[\mathrm{D}_3^b]/C_p}{([\mathrm{D}_1^b]/C_p)^3} \tag{13}$$

$$2\mathrm{D}_3^b \rightleftharpoons \mathrm{D}_6^b, \quad K_2 = \frac{[\mathrm{D}_6^b]/C_p}{([\mathrm{D}_3^b]/C_p)^2} \tag{14}$$

The minimized S value for each scheme is listed in Table 3. In both CV– and TF–NaPP systems, the S value for Scheme III is the smallest among the four schemes and smaller than the preset upper limit of S, and all the corresponding concentrations and ε values are positive. The values of S for the formation of the trimer and the hexamer were extremely large whenever the $\boldsymbol{t}$ matrix gave positive values to the elements of the concentration matrix, $\boldsymbol{C}$.

The fractions of the bound monomer, f_1^b, and the bound dimer, f_2^b, of AA and the fractions of the bound monomer, the bound dimer, and the bound tetramer, f_4^b, of CV and TF obtained from $\boldsymbol{C}$ matrix are plotted as functions of P/D in Figs. 4(a)—(c). The equilibrium constants are listed in Table 4. In Fig. 4, the solid curves show the value of the fractions which were obtained by the Newton method with the values of K for AA or K_1 and K_2 for CV and TF by solving Eq. 6 ($n=2$ for AA) and Eqs. 11 and 12 (for CV and TF) at a given P/D ratio for the concentrations. In the AA–NaPP system, the fraction of the bound monomer increases and that of the bound dimer decreases with the increase in the P/D value. In both the CV– and TF–NaPP systems, the fraction of the bound monomer increases with the increase in P/D and that

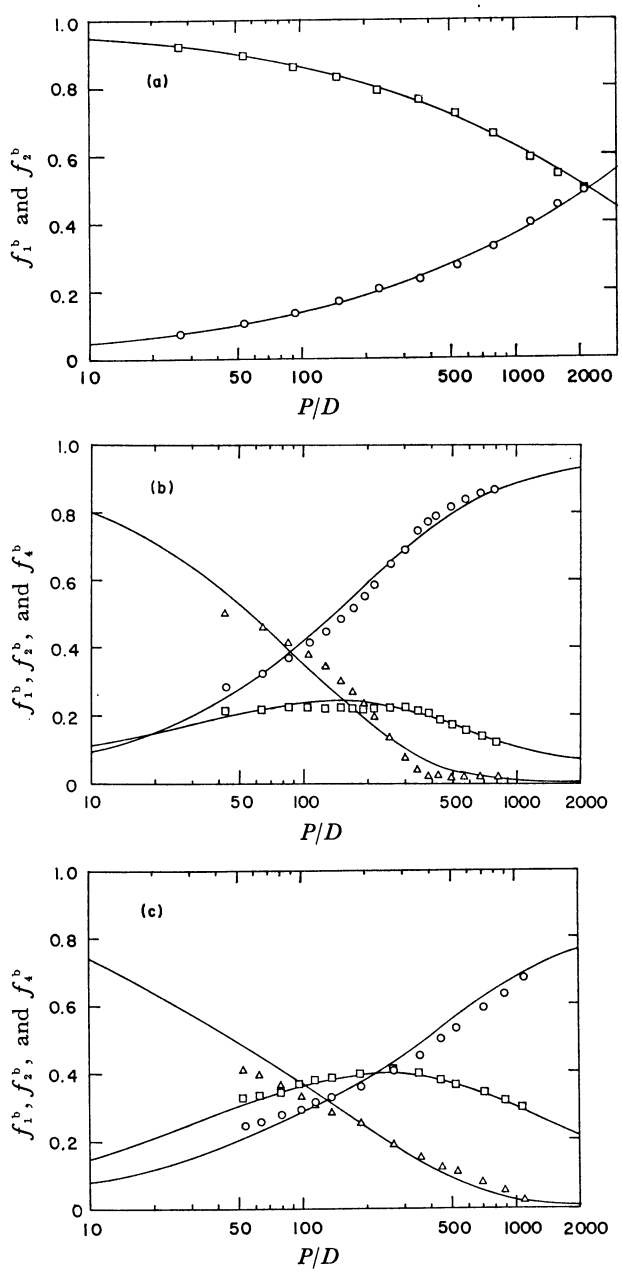

Fig. 4. Variation in the fraction of bound dye species with P/D for (a) AA–, (b) CV–, and (c) TF–NaPP systems.
○: Bound monomer, □: bound dimer, and △: bound tetramer.

of the bound dimer shows a maximum at a P/D value of *ca.* 200. The fraction of the bound tetramer tends to increase with the decrease in P/D.

The pure absorption spectra of bound-dye species of AA, CV, and TF thus obtained are shown in Figs. 5(a)—(c). In all the systems, a slight bathochromic shift is observed in the spectrum of the bound monomer. The absorption spectrum of the bound dimer of AA shows hypochromism and a bathochromic shift, while that of the bound dimer and tetramer of CV and TF has absorption bands at both shorter and longer wavelengths than the position of the main band of the free dye. It is noteworthy that the absorption spectrum of the bound dimer of AA and the bound tetramers of CV and TF excellently fits that of the bound-dye species obtained in the low-P/D region.[4,29]

The UV absorption spectrum of the bound monomer and dimer of AA shown in Fig. 1(b) was calculated from three observed spectra, while the fractions of the bound monomer and dimer were obtained from Fig. 4(a) by the least-squares method using the following equation:

$$\varepsilon_\lambda = f_1^b \varepsilon_\lambda^1 + f_2^b \varepsilon_\lambda^2, \tag{15}$$

where ε_λ^1 and ε_λ^2 denote the molar absorption coefficients of the monomer and the dimer respectively and where ε_λ denotes the apparent molar absorption coefficient of the observed spectrum at the λ wavelength. In the UV range, the absorption spectrum of the bound monomer shows a slight bathochromic shift, while that of the bound dimer shows hypochromism and a bathochromic shift, as is observed in the visible-wavelength range.

Discussion

The Number of Bound-dye Species over a Wide P/D *Region.* In order to interpret the metachromasy, a model in which the dyes are bound cooperatively to polyelectrolyte has been used. According to the model, the spectral changes of the dye-polymer solution are attributed to the change in the distribution of dyes on the polymer. Several quantitative expressions[10,24,25] have been used for the distribution of dyes on the polymer chain, assuming that the aggregated dyes interact with the nearest neighbor bound dye. The cooperative binding model implies that the mean aggregation number depends on the P/D (*cf.* Eq. 22 in Ref. 10 and Eq. 22 in Ref. 25), so that a large number of bound-dye species are expected in the wide P/D region. Hence, in order to examine whether or not the cooperative-binding model expresses the metachromatic phenomena correctly, the number of bound-dye species has to be ascertained over a wide P/D region.

The application of the PCA method to the absorption spectra observed over a wide P/D region clearly revealed that there are only two bound-dye species for AA and only three for CV and TF. These results contradict the results expected from the cooperative-binding model.

Equilibrium Scheme of the Binding of Dye to NaPP. In this study, the bound dyes were assumed to be condensed near the polyelectrolyte. Therefore, the equilibrium scheme of the bound monomer⇌bound aggregate in the vicinity of the polymer molecule was examined by the extended PCA method. As is shown in Fig. 4, the agreement between the experimental and calculated data for the fraction of the respective bound-dye species is reasonably good. This means that the simple equilibrium equation expressed by Eq. 5 can be adopted to represent the metachromatic phenomena observed in the high-P/D region.

In a previous report,[4] the equilibrium constant for the binding of a dye to a polyelectrolyte in the low-P/D region less than unity was expressed as follows:

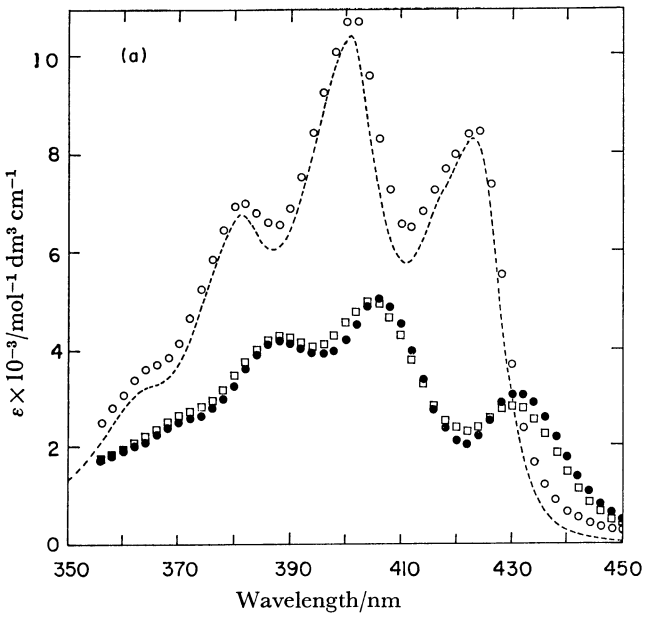

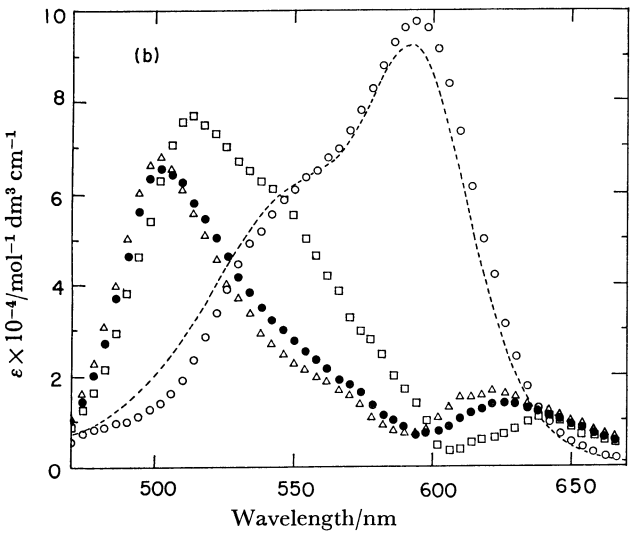

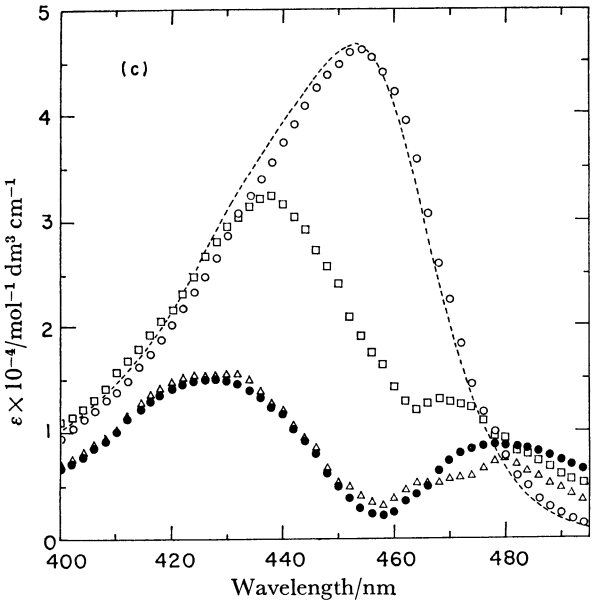

Fig. 5. Pure absorption spectra of bound dyes of AA (a), CV (b), and TF (c).
○: Bound monomer, □: bound dimer, and △: bound tetramer. The absorption spectrum of free dye and bound dye spectrum obtained in the low P/D region are shown by dashed curve and closed circles respectively.

$$K = \frac{[\text{complex}]}{[\text{free dye}][\text{unoccupied binding site}]^{\alpha}}, \tag{16}$$

where α is an empirical parameter. This equation may represent the distribution of the free dye and the total condensed dye in a solution; then the equilibrium constant for the formation of an aggregate in the vicinity of the polymer may be expressed by Eq. 6. Therefore, the amount of dye molecules represented as a complex in Eq. 16 is equal to the sum of the dye molecules of the respective bound-dye species. The fraction of the bound dimer of AA and that of the bound tetramers of CV and TF tends to increase up to unity in the low-P/D region, as is shown in Fig. 4. Hence, the amount of the dye molecules of the complex in Eq. 16 is nearly equal to that of the bound dimer for AA and that of the bound tetramers for CV and TF in the low-P/D region. This is consistent with the fact that the spectrum of the bound dimer of AA and that of the bound tetramers of CV and TF fits into the spectrum of the bound-dye species obtained in the low-P/D region. That is, the bound dimer of AA and the bound tetramers of CV and TF may be primarily present in the low-P/D region. Pal and Mandel[31] also suggested, for the pynacyanol–poly(L-glutamic acid) system, that dyes bound to a long polymer chain may form several small stacks, primarily tetra- and pentamer.

Equation 6 can be express another equilibrium scheme when the equation is rewritten with attention to the counter ion of the polyelectrolyte. In the polyelectrolyte solution without any added salt, the concentration of counter ions, for example, that of Na of NaPP, is equal to that of the polymer residues, so that Eq. 6 can be rewritten as follows:

$$K = \frac{[\mathrm{D}_n^{\mathrm{b}}][\mathrm{Na}]^n}{[\mathrm{D}_1^{\mathrm{b}}]^n[\mathrm{Na}]} = \frac{[\mathrm{D}_n^{\mathrm{b}}][\mathrm{Na}]^{n-1}}{[\mathrm{D}_1^{\mathrm{b}}]^n}. \tag{17}$$

In a previous report,[5] it was clarified that the fraction of bound CV and TF at a P/D, for example, $P/D=1$, increases with an increase in the chain length of NaPP. It was also reported that the amount of bound Na increases with an increase in the chain length of NaPP.[32] These facts suggest that the polyelectrolyte condenses not only the dyes, but also the counter ions, near it and that complexes are formed with the polymer residues, the dyes and the counter ions. Therefore, if it can be assumed that the dyes are bound to the polymer by the Na, Eq. 17 can be rewritten as follows:

$$K = \frac{[\mathrm{NaD}_n^{\mathrm{b}}][\mathrm{Na}]^{n-1}}{[\mathrm{NaD}_1^{\mathrm{b}}]^n}. \tag{18}$$

That is, this equation represents the following scheme:

$$n\mathrm{NaD}_1^{\mathrm{b}} \rightleftharpoons \mathrm{NaD}_n^{\mathrm{b}} + (n-1)\mathrm{Na} \tag{19}$$

where n bound monomers, which are bound to the

polymer by an Na, form the *n*-mer bound to the polymer by an Na. The participation of sodium in the formation of the dye–polyelectrolyte complex might be represented by the empirical parameter, α, introduced into Eq. 16, as has previously been mentioned.[4,5] The participation of sodium in the metachromasy could not be examined by the PCA method; however, it may be examined by means of electrochemical measurements, such as electrophoretic, potentiometric, and conductometric measurements.[2,3,33]

The Pure Spectrum and Structure of Bound-dye Species. The pure spectra of bound-dye species could be obtained for AA, CV, and TF by the application of the extended PCA method to a set of absorption spectra observed over a wide P/D region. It was revealed that the absorption spectra of the bound monomers of AA, CV, and TF show a slight bathochromic shift. The visible and UV absorption bands of AA, CV, and TF are attributable to the π-π^* transition.[34,35] The bathochromic shift of the π-π^* transition is generally induced by interaction with the polar solvent or the formation of a hydrogen bond.[36] Therefore, the bathochromic shift observed for the bound monomer may be due to the interaction between the dye and the ionized group of NaPP. The observed bathochromic shift is very small, so that it may be thought that the dye in monomeric form is loosely bound to NaPP and moves in its vicinity. Yamaoka and Noji[37] reported a sharp triplet line in the ESR spectrum of the spin-labeled proflavine–NaPP system at $P/D=200$; this also suggests that a bound-dye species rotates or moves rapidly.

The absorption spectrum of the bound dimer of AA shows a bathochromic shift, while those of the bound dimer and tetramer of CV and TF have absorption bands at wavelengths both shorter and longer than the position of the main band of the free dye. According to the exciton theory for metachromasy,[38] the relations between the position of the metachromasy bands and the orientation of the transition moments in a dye oligomer have been classified into three categories: (i) a parallel side-by-side orientation of the particular transition moments gives rise to the band on the shorter-wavelength side of the transition characterizing the monomer, (ii) an asymmetric oblique orientation gives rise to two bands, on both shorter- and longer-wavelength side, and (iii) a head-to-tail orientation gives rise to a band on the longer-wavelength side. Both the visible and UV absorption spectra of the bound dimer of AA show a bathochromic shift. The visible and UV transition moments of the monomer-free AA are at right angles.[21,28] If a pair of transition moments of AA is oriented head-to-tail in a dimer so as to have a band on the longer-wavelength side, the other pair of transition moments must be oriented side-by-side so as to have a band on the shorter-wavelength side. That is, the relation between the position of the metachromasy bands and the orientation of the transition moment in the dimer of AA is not classified into any category.

The position and number of metachromasy bands may be related to the symmetry of the dye structure, because the absorption spectrum of spin-labeled proflavine, in which the two-fold symmetry of proflavine is distorted by the spin-labeling to an amino group, has two bands, at wavelengths both shorter and longer than the position of the main band of proflavine,[29] while that of doubly spin-labeled proflavine, which is labeled at two aminogroups and which has a two-fold symmetry, has a band on the shorter-wavelength side.[39] Therefore, the absorption spectrum of a dye may have bands at wavelengths both shorter and longer than the position of the original band when the symmetry of the dye is sufficiently distorted. On the other hand, when the symmetry characterizing the monomer dye is not distorted sufficiently by the interaction between the dye and another substance, the absorption spectrum may show only a shift, without any new band. Therefore, the model of the bound dimer shown in Fig. 6 was considered for AA, CV, and TF. In the model, it was assumed that two dye molecules are combined not only by hydrophobic interaction, but also by the interaction between positively charged nitrogen and amino or dimethylamino nitrogen. Then, each of the two dyes has a two-fold symmetry in AA, while the symmetry of the monomer dye is distorted in the dimers of CV and TF.

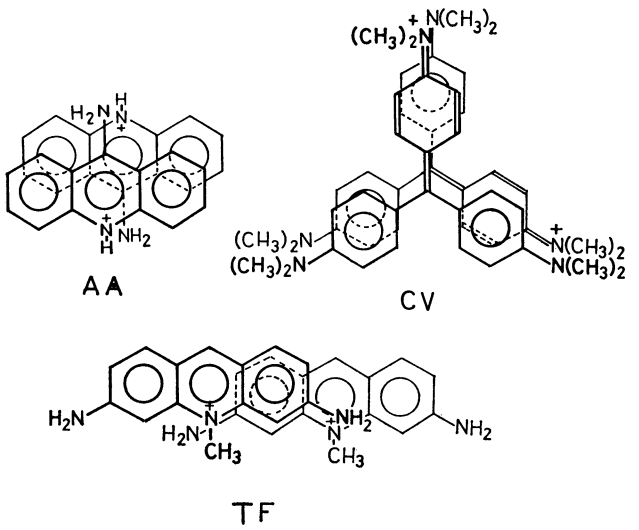

Fig. 6. Schematic model of bound dimer.

The symmetry in the bound tetramer may be more heavily distorted than that in the dimer, because the absorption band located on the shorter-wavelength side shows a larger hypsochromic shift in the bound tetramer than in the bound dimer, as is shown in Figs. 5(b) and (c). The bound tetramers of CV and TF may be more attracted than the monomer by the NaPP because of the four postively charged nitrogen atoms. Therefore, the conformation of the bound aggregate may depend on the backbone structure of the polymer, such as the mean distance between the functional groups of the polymer. Hence, the position and intensity of the absorption bands of the bound-dye species may depend on the polymers, as has previously been mentioned.[4]

For a quantitative discussion of the position of metachromasy bands, however, information is necessary on the electronic states and transition moments of the

aggregated dyes. The LCAO calculation may provide such information. Since the extended PCA method is powerful in a multicomponent system, its application to a series of absorption spectra of dye–polyelectrolyte systems at various temperatures or ionic strenghts should yield information leading to a fuller understanding of metachromasy.

Conclusion

The number of bound-dye species was determined to be two for the AA–NaPP system and three for the CV– and TF–NaPP systems. Using a simple model, in which the condensation of dyes near the polymer is assumed, the equilibrium constant, aggregation number, and pure absorption spectra of the bound-dye species were determined by the extended PCA method. The spectrum of the bound monomer shows a slight bathochromic shift in all cases. The absorption spectrum of the bound dimer of AA shows a considerable bathochromic shift. On the other hand, the absorption spectra of the bound dimer and tetramer of CV and TF have absorption bands at wavelengths both shorter and longer than the position of the main bands of free CV and TF.

The author wishes to express his hearty gratitude to Assistant Professor Kiwamu Yamaoka of Hiroshima University for his helpful discussions and continuous encouragement in the course of this study.

References

1) K. Yamaoka, T. Suenaga, A. Fujita, and M. Miura, *J. Sci., Hiroshima Univ., Ser. A*-II, **34**, 1 (1970).
2) K. Yamaoka, M. Takatsuki, K. Yaguchi, and M. Miura, *Bull. Chem. Soc. Jpn.*, **47**, 611 (1974).
3) K. Yamaoka, M. Takatsuki, and M. Miura, *Bull. Chem. Soc. Jpn.*, **48**, 2739 (1975).
4) K. Yamaoka and M. Takatsuki, *Bull. Chem. Soc. Jpn.*, **51**, 3182 (1978).
5) M. Takatsuki and K. Yamaoka, *Bull. Chem. Soc. Jpn.*, **52**, 1003 (1979).
6) K. Yamaoka and M. Masujima, *Biopolymers*, **17**, 2485 (1978).
7) T. Soda and K. Yoshioka, *Nippon Kagaku Zasshi*, **87**, 22 (1966).
8) G. Schwarz, S. Klose, and W. Balthasar, *Eur. J. Biochem.*, **12**, 454 (1970).
9) V. Vitagliano and L. Costantino, *J. Phys. Chem.*, **74**, 194 (1970).
10) V. Vitagliano, L. Costantino, and A. Zagari, *J. Phys. Chem.*, **77**, 204 (1973).
11) V. Vitagliano, L. Costantino, and R. Sartorio, *J. Phys. Chem.*, **80**, 959 (1976).
12) W. H. J. Stork, P. L. de Hasseth, W. B. Shippers, C. M. Kormeling, and M. Mandel, *J. Phys. Chem.*, **77**, 1772 (1973).
13) M. Shirai, T. Nagatsuka, and M. Tanaka, *Makromol. Chem.* **178**, 37 (1977).
14) G. Weill and M. Calvin, *Biopolymers*, **1**, 401 (1963).
15) V. Kleinwächter and J. Koudelka, *Biophysik*, **5**, 119 (1968).
16) G. Löber, J. Koudelka, and E. Smékal. *Biophys. Chem.*, **2**, 158 (1974).
17) Z. Balcarova, V. Kleinwächter, J. Koudelka, R. Klarner, and G. Löber, *Biophys. Chem.*, **8**, 17 (1978).
18) G. Löber and G. Achtert, *Biopolymers*, **8**, 595 (1969).
19) R. K. Tubbs, W. E. Ditmars, Jr., and Q. Van Winkle, *J. Mol. Biol.*, **9**, 545 (1964).
20) K. Yamaoka, *Biopolymers*, **11**, 2537 (1972).
21) K. Jakson and S. F. Mason, *Trans. Faraday Soc.*, **69**, 966 (1971).
22) R. W. Armstrong, T. Kurucsev, and U. P. Strauss, *J. Am. Chem. Soc.*, **92**, 3174 (1970).
23) M. Takatsuki and K. Yamaoka, *J. Sci. Hiroshima Univ., Ser. A*, **40**, 387 (1976).
24) D. F. Bradley and M. K. Wolf, *Proc. Natl. Acad. Sci., U. S. A.*, **45**, 944 (1959).
25) G. Schwarz, *Eur. J. Biochem.*, **12**, 442 (1970).
26) K. Yamaoka and R. A. Resnik, *Biopolymers*, **8**, 289 (1969).
27) K. Yamaoka, T. Matsuda, and M. Takatsuki, *Bull. Chem. Soc. Jpn.*, **53**, 968 (1980).
28) W. Seiffert, V. Zanker, M. Mantsch, and B. Schneider, *Tetrahedoron Lett.*, **54**, 5655 (1968).
29) K. Yamaoka, M. Takatsuki, and K. Nakata, unpublished.
30) F. Oosawa, "Polyelectrolytes," Marcel Dekker, New York (1971), Chap. 2.
31) M. K. Pal and M. Mandel, *Biopolymers*, **18**, 2267 (1979).
32) U. Schindewolf, *Z. Phys. Chem.*, **1**, 134 (1954).
33) F. Watanabe, *Bull. Chem. Soc. Jpn.*, **49** 1465 (1976).
34) Y. Matsuoka and K. Yamaoka, *Bull. Chem. Soc. Jpn.*, **52**, 2244 (1979).
35) Y. Matsuoka and K. Yamaoka, *Bull. Chem. Soc. Jpn.*, **52**, 3163 (1979).
36) H. H. Jaffé and M. Orchin, "Theory and Applications of Ultraviolet Spectroscopy," John Wiley and Sons, Inc., New York (1966), p. 186.
37) K. Yamaoka and S. Noji, *Chem. Lett.*, **1976**, 1355.
38) D. F. Bradley, I. Tinoco, Jr., and R. W. Woody, *Biopolymers*, **1**, 239 (1963).
39) K. Yamaoka and S. Noji, *Chem. Lett.*, **1979**, 1123.